

Original Research Paper

Reversible Ionizing Radiation Sensors Based on Carbon Nanotubes

¹Kenneth Fontáñez, ²Abniel Machín, ¹María C. Cotto,
¹José Duconge, ³Carmen Morant and ¹Francisco Márquez

¹Nanomaterials Research Group-NRG, Department of Chemistry and Physics, School of Natural Sciences and Technology, Universidad Ana G. Méndez-Gurabo Campus, 189 St. Rd. km 3.3, 00778-Gurabo, PR, USA

²Department of Chemistry, University of Puerto Rico, Río Piedras Campus, 17 Ave. Universidad, 00925-San Juan, PR, USA

³Department of Applied Physics, Universidad Autónoma de Madrid, 28049-Cantoblanco, Madrid, Spain

Article history

Received: 14-01-2020

Revised: 28-01-2020

Accepted: 01-02-2020

Corresponding Author:

Francisco Márquez

Nanomaterials Research Group-NRG, Department of Chemistry and Physics, School of Natural Sciences and Technology, Universidad Ana G. Méndez-Gurabo Campus, 189 St. Rd. km 3.3, 00778-Gurabo, PR, USA

Email: fmarquez@uagm.edu

Abstract: Vertically Aligned Carbon Nanotubes (VA-CNTs) were grown by Chemical Vapor Deposition (CVD) on a silicon substrate with alternating layers of TiN and SiO₂. VA-CNTs were exposed to X-ray radiation to study the change in resistivity later. Preliminary results show an increase in the resistivity of CNTs as a function of radiation exposure time, which means that the structure responds successfully to radiation exposure. The variation of resistivity has been associated with the presence of organic compounds that, during exposure to radiation, can generate species capable of interacting with the material by modifying its conductive properties. The first evidence indicates that the changes observed are reversible under heat treatment, which also supports the fact that it is the adsorbed organic species that, in the presence of radiation, modify the resistivity of the material and possibly allowing the material to be recyclable.

Keywords: Vertically Aligned Carbon Nanotubes, Radiation, Sensor, Resistivity

Introduction

Ionizing radiation is characterized by its ability to excite and ionize atoms of matter with which it interacts (Andreo *et al.*, 2017). Biological systems (e.g., humans) are particularly susceptible to damage by ionizing radiation, so that the expenditure of a relatively trivial amount of energy ($\sim 4 \text{ J kg}^{-1}$) throughout the body could cause death, although that amount of energy can only raise the gross temperature by about 0.001°C (Andreo *et al.*, 2017). Clearly, the ability of ionizing radiation to impart energy to individual atoms, molecules and biological cells has a profound effect on the outcome and that is why the detection is crucial in different fields, including energy, national security, emergency response, medical research and therapy, nuclear research and space exploration (Kim *et al.*, 2019). Some radiation detectors consist of various materials such as graphene (Serry *et al.*, 2015), tin (Sn) (Kim *et al.*, 2019), SiC (Tripathi *et al.*, 2019), germanium (Rahman *et al.*, 2015) and others. In these cases, the measurements are based on the microcalorimetry of some actinides (Chavan *et al.*, 2016), scintillation (Yanagida, 2016), thermoluminescence

(Bortolin *et al.*, 2019) or detection by photoelectric effect (Mizanur-Rahman *et al.*, 2015). All these systems are characterized by being volume based, which implies that large systems are needed to carry out sufficiently reliable radiation measurements (Kozlovskiy *et al.*, 2019). Faced with these limitations, the incorporation of nanomaterials, capable of experiencing sufficiently measurable changes, could be a realistic alternative, especially for advanced portable devices (Karthick-Kannan *et al.*, 2015; Márquez and Morant, 2015).

One of the characteristics of carbon nanotubes, especially Single-Walled carbon Nanotubes (SWNT), is that the conductive properties vary greatly depending on the presence of defects in the structure, or also of adsorbed or bonded species (Yang *et al.*, 2016; Zaporotskova *et al.*, 2016). The presence of small defects in the walls of the nanotubes, or what is the same, the lack of a single atom, or even the incorporation of a molecule or the interaction with any structure, can generate a local change in the electronic distribution that will produce alterations in the conductive properties of the nanotubes (Kim *et al.*, 2016; Fang *et al.*, 2017; Zhang *et al.*, 2017). These changes will be much greater

the more relevant the changes produced in the structure of the nanotube. These defects, or the interaction with molecules present in the nanotube environment, can be induced by the presence of ionizing radiation. As described in previous work (Fontáñez *et al.*, 2019), ionizing radiation produces alterations in the structure of nanotubes that could be correlated with radiation doses. These changes have been observed by Raman spectroscopy, XPS and by means of resistivity measurements of the material. In this investigation, vertically aligned carbon nanotubes were grown by Chemical Vapor Deposition (CVD) on a silicon oxide substrate with alternate layers of Titanium Nitride (TiN). The Carbon Nanotubes (CNTs) were exposed to different doses of X-ray radiation to study the alterations produced in the presence of organic compounds. The results obtained show an increase in the resistivity of the CNT as a function of the radiation exposure time. The changes observed are reversible under heat treatment, so these materials could be used as radiation sensors even for relatively low doses and energies.

Experimental Section

Reagents and Preparation of Substrates

All chemicals used in this investigation were analytical grade and were used as received, without further purification. Ethyl alcohol (99.99%, 200 proof), cobalt (Co) and molybdenum (Mo) salts ($\text{Co}(\text{CH}_3\text{COO})_2 \cdot 4\text{H}_2\text{O}$ and $\text{Mo}(\text{CH}_3\text{COO})_2$), acetone (HPLC, >99.9%) and methanol (HPLC, >99.9%) were provided by Sigma Aldrich Corp. (MO, USA). Isopropyl alcohol (99.9%) was provided by Fisher Scientific. Si wafers (Si <100>, 300 μm thick, type p, single-sided polishing), were provided by El-CAT Inc. and were used as substrates. TiN target (99.99%) was provided by Goodfellow Cambridge Ltd. Deionized water was used for all experiments (Milli-Q, resistivity of 18.2 $\text{M}\Omega \cdot \text{cm}$ at 25°C). Ultra-high purity nitrogen gas (99.999%) and ultra-high purity hydrogen gas (99.99%) were provided by Praxair.

The substrate preparation process has been described elsewhere (Fontáñez *et al.*, 2019). According to this procedure, Si<100> substrates, cleaned with acetone and isopropyl alcohol, were dried under nitrogen flow. Then, substrates were subjected to a heat treatment at 200°C for 5 minutes and under vacuum (10^{-3} mbar) to obtain a layer of thermal Silicon Oxide (SiO_2) of ca. 200 nm (according to SEM measurements). Next, SiO_2 @Si substrates were coated with TiN by Physical Vapor Deposition (PVD). For this, a TiN target was used. The optimized deposition temperature was 120°C, with a deposition time of 80 min and a TiN thickness of ca. 90 nm. The specific pattern of alternative regions of TiN and SiO_2 was obtained by sputtering with an ion gun

(Ion Tech Inc., 600 V and 10^{-4} mbar pressure), using a micrometric-sized patterned mask.

The deposition of Co-Mo catalysts was carried out by dip-coating with solutions of $\text{Co}(\text{CH}_3\text{COO})_2 \cdot 4\text{H}_2\text{O}$ (0.02% v/v in ethanol) and $\text{Mo}(\text{CH}_3\text{COO})_2$ (0.04% v/v in ethanol) (Morant *et al.*, 2012). The substrates are then calcined in the air at 400°C for 20 min. As a result, these catalysts will be in oxidized form. However, during the SWNT growth process, the oxides of Mo and Co will be reduced to their metallic forms.

Growth of SWNTs

The synthesis of SWNT was carried out through the use of a Chemical Vapor Deposition (CVD) system, described elsewhere (Fontáñez *et al.*, 2019) and composed of a three-input cylindrical quartz reactor with an internal diameter of 25 mm and a length of 1 m, installed inside a tubular oven. The substrates based on TiN-SiO_2 @Si<100>, whose synthesis was described above, were introduced into the reactor. Then, the substrates were heated under vacuum of $5 \cdot 10^{-3}$ mbar for 30 min. Next and while the reactor is heated to 1123 K (5°C min^{-1}), a mixture of N_2 (300 sccm) and H_2 (50 sccm) is incorporated. Once the final temperature is reached, the flow of N_2 is replaced by N_2 saturated with ethanol: water (99.5:0.5 v/v). For this, the N_2 is bubbled over an ethanol-water container previously heated to 40°C and with an overpressure of 0.5 bar. Finally, the synthesis is completed by interrupting the flow of reactive gases and replacing them with a flow of N_2 until reaching room temperature (Fig. 1).

Characterization Techniques

The samples were characterized by Field Emission Scanning Electron Microscopy (FE-SEM), using a JEOL JM6400, which operates at 20 kV. X-ray Photoelectron Spectroscopy (XPS) was measured with an ESCALAB 220i-XL spectrometer, using a non-monochromatic Mg $K\alpha$ radiation (1253.6 eV) from a twin anode, operating at 20 mA and 10 kV in the constant analyzer energy mode, using a PE of 40 eV. Raman spectra were obtained with a Renishaw spectrometer equipped with a 532 nm laser at 8 mW and a nominal resolution of 5 cm^{-1} . The exposure of SWNT samples to ionizing radiation (X-rays) was performed using an X-ray diffractometer, X-Pert PRO, using Cu- $K\alpha$ radiation ($\lambda = 1.5418 \text{ \AA}$, 40 kV, 40 mA) and incidence angle of 90° . Resistivity measurements were carried out using a two-probe conductivity cell at 20°C. To do this, the samples were treated as follows: (i) activation at 200°C for 1 h, in vacuum (100 mm Hg); and (ii) incorporation of a mixture of acetone: methanol (1:1, v/v), by bubbling with N_2 for 5 min in a reduced pressure system (100 mm Hg). Next, the resistivity measurements were performed before and after desorption treatments at 50°C, 100°C and 150°C under vacuum (100 mm Hg) for 30 min.

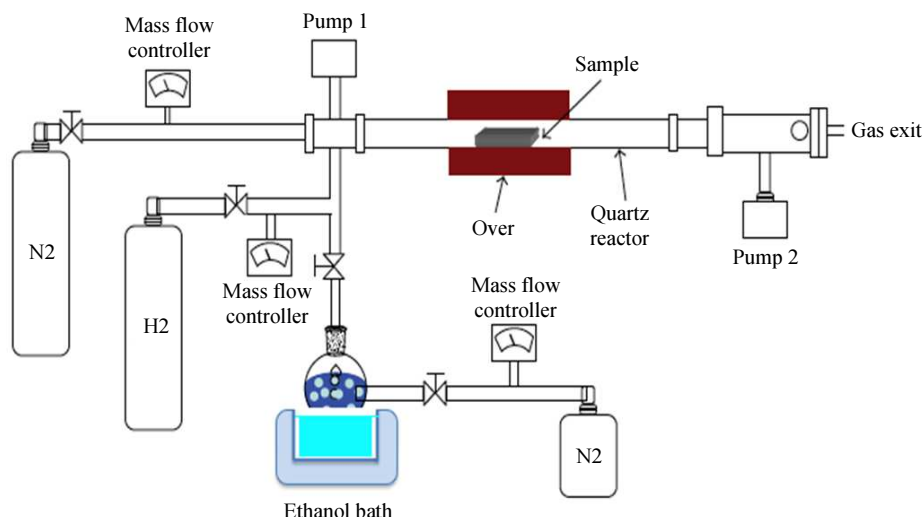


Fig. 1: CVD assembly used in this research

Results and Discussion

As described in a previous paper (Fontánez *et al.*, 2019), the growth of SWNTs using TiN-SiO₂@Si<100>-based substrates is only observed on the SiO₂ lanes. Figure 2 shows the SEM image of the as-synthesized carbon nanotubes. The right side of Fig. 2 clearly shows the vertical orientation of the carbon nanotubes obtained according to the procedure described. The nanotubes obtained are characterized by having a very low level of defects and an average diameter that is around 1.3 nm. This starting material is what has been used to study the effects of X-ray radiation on the structure.

In previous work (Fontánez *et al.*, 2019), it was observed that the exposure of SWNT to X-rays increased the resistivity of the material and the resistivity depended on the time of exposure to X-rays. Additionally, it was speculated with the possibility that the organic species adsorbed could interact with the nanotubes due to the effect of radiation, generating the observed change in electronic properties. In order to verify these hypotheses, samples of VA-SWNTs were subjected to X-rays (40 KV, 40 mA), after being treated at 400°C and vacuum (10⁻³ mbar) for 2 h. Figure 3a shows that, under these conditions, no apparent changes in the resistivity of the material were observed. However, these changes were evident when the material was previously exposed to the vapors of a mixture of acetone-methanol (Fig. 3b-e). Figure 3b shows the resistivity of the material exposed to acetone-methanol vapors, without heat treatment or under vacuum to remove excess adsorbed organic material. As it can be seen, the resistivity gradually increases from 100 to more than 1300 as a function of the exposure time to X-rays. In the case of samples

treated at different temperatures (50°C, 100°C and 150°C) and vacuum (Fig. 3c-e) for 1 hour, to eliminate part of the organic adsorbed on the surface of the material, variations of smaller magnitude are observed that clearly correlate with the level of organic matter present on the surface of the sample.

In order to test the reversibility of the changes observed in the resistivity of the material, the sample exposed to organic and which was not treated at temperature before exposure to X-rays (Fig. 3b), was treated at 400°C and vacuum for 2 h (Fig. 4). This sample was then subjected to different exposure times with X-rays and resistivity evaluation. As can be seen, the resistivity did not undergo an appreciable variation after 4 hours of exposure to X-rays (Fig. 4a). This same sample was then exposed to organic (Fig. 4b), using the process described above, observing a behavior similar to that described in Fig. 3b.

The observed changes in the resistivity of the material were also characterized by XPS. Figure 5 shows the transitions corresponding to C1s and O1s of the sample exposed to organic and that was not irradiated, as well as the result after exposing the sample to 2 hours and 4 hours to X-rays. In the sample not exposed to radiation, both transitions show symmetrical peaks and apparently only one component. In the case of C1s, a peak centered at ca. 284.5 eV, characteristic of the carbon in graphitic structure, is observed. The O1s shows a peak centered at ca. 531.5 eV that can be assigned to the presence of O-C bonds (Briggs and Seah, 1994), possibly in terminal regions of the nanotubes. After 2 h of exposure to X-rays, both transitions show a slightly asymmetric widening. C1s shows a new component at approximately 286.1 eV, which has been associated with the incorporation of oxygenated species.

In the case of O1s, a similar behavior is observed, with the presence of a new component at ca. 533.2 eV, associated with the presence of OH- groups or even hydroxyl radicals on the surface (Briggs and Seah, 1994). This widening of transitions C1s and O1s is even more marked after 4 h of exposure to X-rays (Fig. 5).

The samples analyzed by XPS were also characterized by Raman spectroscopy (Fig. 6). As can be seen there, the sample not exposed to radiation shows the G and D bands at 1585 cm^{-1} and 1360 cm^{-1} , respectively. The high intensity ratio of the G band to the

D band (G/D ratio) reflects the purity of the nanotubes, with a low level of defects (Dresselhaus *et al.*, 2005). The small peak below 300 cm^{-1} , corresponding to Radial Breathing Modes (RBM), can be associated with the presence of nanotubes of homogeneous diameter of ca. 1.3 nm (Dresselhaus *et al.*, 2005). When the material is exposed to radiation, a slight increase in the D-band is observed, which is associated with the presence of structural defects. This increase in intensity, although weak, is even greater after submitting the sample to 4 h of exposure to X-rays (see inset of Fig. 6).

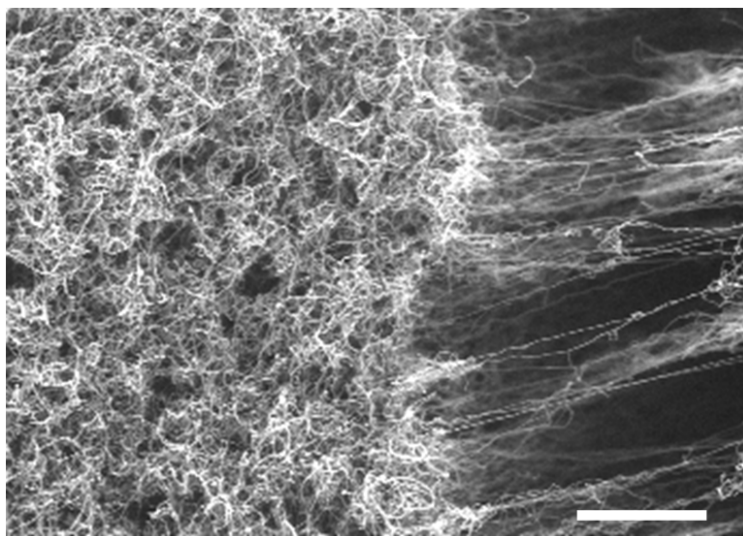


Fig. 2: SEM image of the VA-SWNTs grown on the SiO₂ lanes (scale bar is 1 μm)

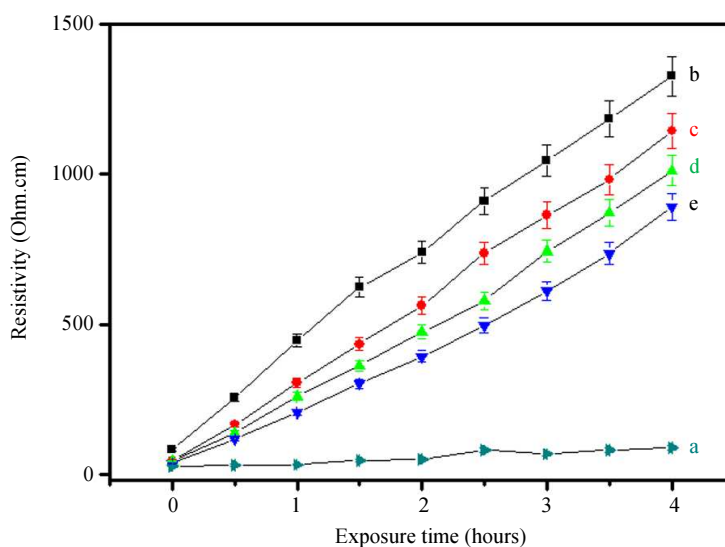


Fig. 3: Variation of the average resistivity as a function of the exposure time to X-rays after treatment at 400°C and vacuum for 2 h (a); after exposure to organic (b); after exposure to organic and thermal treatment at 50°C and vacuum for 1 h (c); after exposure to organic and thermal treatment at 100°C and vacuum for 1 h (d); and after exposure to organic and thermal treatment at 150°C and vacuum for 1 h

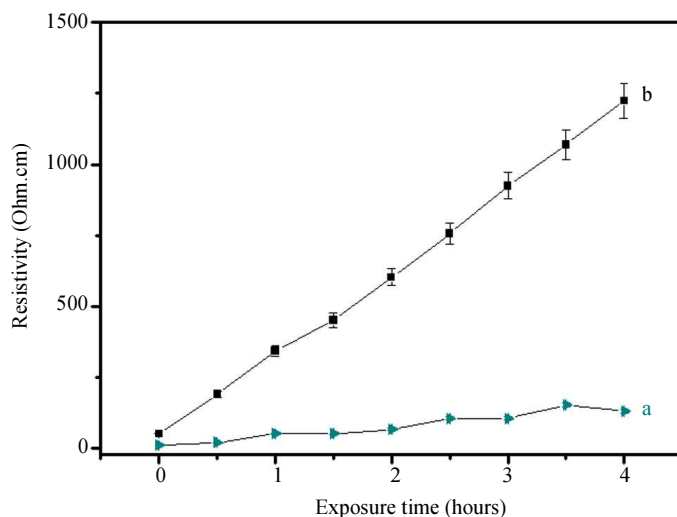


Fig. 4: Variation of the average resistivity as a function of the time of exposure to X-rays after treatment at 400°C and vacuum for 2 h (a) and after exposure to organic (b)

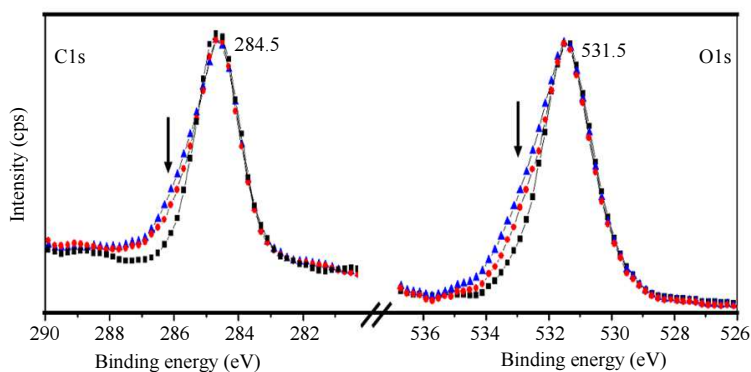


Fig. 5: C1s and O1s XPS peaks of the as-synthesized SWNTs (black line). The red and blue line spectra correspond to those measured after exposure to X-rays for 2 h and 4 h, respectively

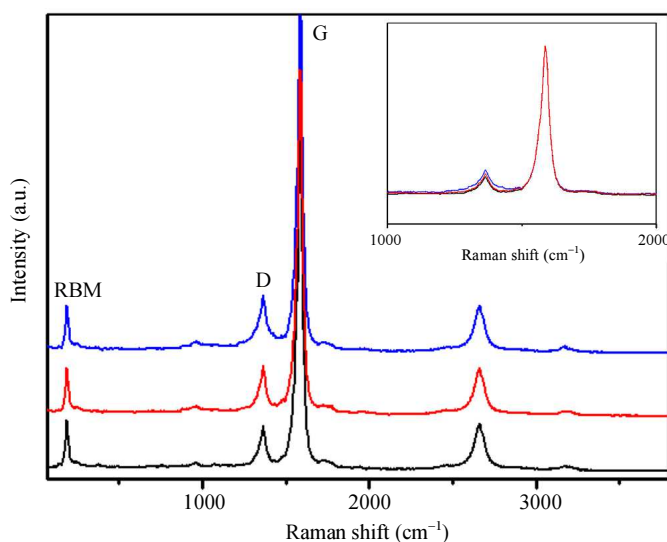


Fig. 6: Raman spectra of the as-synthesized SWNTs (black line) and after exposure to X-ray radiation for 2 hours (red line) and 4 hours (blue line). The inset zooms-in the D and G-bands

Conclusion

In this research, vertically aligned SWNTs were synthesized using CVD and their potential use for sensor development was evaluated. According to the characterization by Raman spectroscopy, these nanotubes show a low level of defects and an average diameter of ca. 1.3 nm. These nanotubes were exposed to vapors of a mixture of acetone-methanol and then subjected to X-ray radiation. The results obtained show a correlation between the resistivity of the material and the exposure time to X-ray radiation. Through XPS it has been shown that the increase in the resistivity of the material occurs together with the appearance of oxidized species that interact with the surface of the material. The first evidence suggests that these species could be radical $\cdot\text{OH}$ or hydroxyl groups, produced during exposure to X-rays. According to the results obtained, these species can be partially eliminated by thermal treatment in vacuum, which could allow the material to be recyclable.

Additional work will be required to fully identify the species that are being produced and that are responsible for this behavior. On the other hand, for future applications it would be interesting to study whether different species can be generated using organic compounds other than those used in this research. If so, materials could be designed for different applications and with different ranges of use.

Acknowledgement

KF thanks The Puerto Rico Louis Stokes Alliance for Minority Participation (PR-LSAMP) for a research scholarship.

Funding Information

Financial support from the U.S. Department of Defense under Grant W911NF-14-1-0046, from MINECO under Grant ENE2014-57977-C2-1-R and from the US Department of Energy and the Consortium for Integrating Energy System in Engineering and Science Education, CIESESE (DENA0003330), is gratefully acknowledged.

Author's Contributions

All authors contributed equally to this work.

Ethics

This article is original and contains unpublished material. The corresponding author confirms that all of the other authors have read and approved the manuscript and no ethical issues involved.

References

- Andreo, P., T.D. Burns, E.A. Nahum, J. Seuntjens and H.F. Attix, 2017. Fundamentals of ionizing Radiation Dosimetry. 1st Edn., Weinheim, Germany, ISBN-10: 3527409211, pp: 1000.
- Bortolin, E., C. De Angelis, M.C. Quattrini, O. Brlascini and P. Fattibene, 2019. Detection of Ionizing Radiation Treatment in Glass used for Healthcare products. *Radiat. Prot. Dosimetry*.
DOI: 10.1093/rpd/ncz014
- Briggs, D. and M.P. Seah, 1994. Practical Surface Analysis: Auger and X-Ray Photoelectron Spectroscopy. 2nd Edn., Wiley, New York.
- Chavan, V., C. Agarwal and A.K. Pandey, 2016. Pore-filled scintillating membrane as sensing matrix for α -emitting actinides. *Anal. Chem.*, 88: 3796-3803.
DOI: 10.1021/acs.analchem.5b04827
- Dresselhaus, M.S., G. Dresselhaus, R. Saito and A. Jorio, 2005. Raman spectroscopy of carbon nanotubes. *Phys. Rep.*, 409: 47-99.
DOI: 10.1016/j.physrep.2004.10.006
- Fang, R., G. Li, S. Zhao, L. Yin and K. Du *et al.*, 2017. Single-wall carbon nanotube network enabled ultrahigh sulfur-content electrodes for high-performance lithium-sulfur batteries. *Nano Energy*, 42: 205-214. DOI: 10.1016/j.nanoen.2017.10.053
- Fontánez, K., A. García, M.C. Cotto-Maldonado, J. Duconge and C. Morant *et al.*, 2019. Development of ionizing radiation sensors based on carbon nanotubes. *Am. J. Eng. Applied Sci.*, 12: 185-192.
DOI: 10.3844/ajeassp.2019.185.192
- Karthick-Kannan, P., D.J. Late, H. Morgan and C. Sekhar-Rout, 2015. Recent developments in 2D layered inorganic nanomaterials for sensing. *Nanoscale*, 7: 13293-13312.
DOI: 10.1039/C5NR03633J
- Kim, J., S.W. Choi, J.H. Lee, Y. Chung and Y.T. Byun, 2016. Gas sensing properties of defect-induced single walled carbon nanotubes. *Sensors Actuators B: Chemical*, 228: 688-692.
DOI: 10.1016/j.snb.2016.01.094
- Kim, J.H., A. Mirzaei, H. Woo-Kim, H. Joo-Kim and P. Quoc-Vuong *et al.*, 2019. A novel x-ray radiation sensor based on networked SnO₂ nanowires. *Applied Sci.*, 9: 4878-4878.
DOI: 10.3390/app9224878
- Kozlovskiy, A.L., M.B. Abdgaliyev, G. Akhtanova and M.V. Zdorovets, 2019. Radiation resistance of thin TiN films as a result of irradiation with low-energy Kr¹⁴⁺ ions. *Ceram. Int.*
DOI: 10.1016/j.ceramint.2019.12.018
- Márquez, F. and C. Morant, 2015. Nanomaterials for sensor applications. *Soft Nanosci. Lett.*, 5: 1-2.
DOI: 10.4236/snll.2015.51001

- Mizanur-Rahman, A.K.M., Zubair, H.T. Mahfuza-Begum, H.A. Abdul-Rashid and Z. Yusoff *et al.*, 2015. Germanium-doped optical fiber for real-time radiation dosimetry. *Radiat. Phys. Chem.*, 116: 170-175.
DOI: 10.1016/j.radphyschem.2015.04.018
- Morant, C., T. Campo, F. Márquez, C. Domingo and J.M. Sanz *et al.*, 2012. Mo-Co catalyst nanoparticles: Comparative study between TiN and Si surfaces for single-walled carbon nanotube growth. *Thin Solid Films*, 520: 5232-5238.
DOI: 10.1016/j.tsf.2012.03.099
- Rahman, A., H. T. Zubair, M. Begum, H. A. Abdul-Rashid, Z. Yusoff, *et al.* 2015. Germanium-doped optical fiber for real-time radiation dosimetry. *Radiation Physics and Chemistry* 116: 170-175.
DOI: 10.1016/j.radphyschem.2015.04.018
- Serry, M., A. Hameed-Sharaf, A. Emira, A. Abdul-Wahed and Gamal, A. 2015. Nanostructured graphene-Schottky junction low-bias radiation sensors. *Sens. Actuators A: Phys.*, 232: 329-340.
DOI: 10.1016/j.sna.2015.04.031
- Tripathi, S., C. Upadhyay, C.P. Nagaraj, A. Venkatesan and K. Devan, 2019. Effects of Electron and Proton Irradiation on the Electrical Characteristics of the SiC-based Fast Neutron Detectors. *JINST*, 14: P02002-P02002.
DOI: 10.1088/1748-0221/14/02/P02002
- Yanagida, T., 2016. Ionizing radiation induced emission: Scintillation and storage-type luminescence. *J. Lumin.*, 169: 544-548.
DOI: 10.1016/j.jlumin.2015.01.006
- Yang, F., X. Wang, M. Li, X. Liu and X. Zhao *et al.*, 2016. Templated synthesis of single-walled carbon nanotubes with specific structure. *Acc. Chem. Res.*, 49: 606-615.
DOI: 10.1021/acs.accounts.5b00485
- Zaporotskova, I.V., N.P. Boroznina, Y.N. Parkhomenko and L.V. Kozhitov, 2016. Carbon nanotubes: Sensor properties. A review. *Modern Electronic Mater.*, 2: 95-105. DOI: 10.1016/j.moem.2017.02.002
- Zhang L., D.M. Sun, P.X. Hou, C. Liu and T. Liu *et al.*, 2017. Selective growth of metal-free metallic and semiconducting single-wall carbon nanotubes. *Adv. Mater.*, 29: 1605719-1605719.
DOI: 10.1002/adma.201605719